

Cite this: *Chem. Sci.*, 2019, 10, 5539

All publication charges for this article have been paid for by the Royal Society of Chemistry

Received 31st January 2019

Accepted 25th April 2019

DOI: 10.1039/c9sc00561g

rsc.li/chemical-science

## Tuning ligand field strength with pendent Lewis acids: access to high spin iron hydrides†

John J. Kiernicki,<sup>a</sup> James P. Shanahan,<sup>a</sup> Matthias Zeller<sup>b</sup>  
and Nathaniel K. Szymczak<sup>id</sup>\*<sup>a</sup>

Geometrically flexible 9-borabicyclo[3.3.1]nonyl units within the secondary coordination sphere enable isolation of high-spin Fe(II)-dihydrides stabilized by boron–hydride interactions and a rare example of an isolable  $S = 3/2$  reduction product. The borane-capped Fe(II)-dihydride: (1) rapidly deprotonates E–H (E = N, O, P, S) bonds to afford borane-stabilized Fe adducts and (2) releases  $H_2$  upon exposure to  $\pi$ -acids. The Lewis acids provide an avenue for redox-leveling in analogy to the near constant operating potential for  $N_2$  reduction in nitrogenase.

Iron-dihydrides are intermediates in myriad homogenous catalytic reactions and the recent push to develop earth-abundant transition metal catalysts has fueled many research groups to explore their reactivity.<sup>1</sup> Beyond relevance to homogenous catalysis, iron-dihydrides have been implicated in biological reduction sequences. Whereas strong-field hydride ligands typically enforce low-spin configurations, metal-locofactors including nitrogenase contain high-spin hydrides.<sup>2</sup> To account for the modest conditions used by nitrogenase enzymes for  $N_2$  reduction, one proposal to accumulate reducing power at a near constant potential is to store reducing equivalents as Fe– $\mu$ -H–Fe intermediates.<sup>2,3</sup> For example, the  $E_4$  state of the FeMoco center of nitrogenase is proposed to eliminate  $H_2$  from accumulated bridging hydrides concomitant with  $N_2$  binding/reduction (Fig. 1).

Well characterized synthetic examples of open-shell Fe– $\mu$ -H–Fe complexes are rare,<sup>4</sup> and thus, despite their relevance in biology, the synthesis and reactivity of such species remain largely unknown. This disparity is likely due to the mismatched requirements of the ligand/metal combination – strong-field hydride donor ligands rarely afford high-spin electronic configurations.

Our group is working to evaluate how the precise structural, electronic, and cooperative modes in the secondary coordination sphere can be used to regulate reactivity.<sup>5</sup> One way in which the ligand-field strength of otherwise strong-field hydride ligands can be attenuated (accommodating high-spin states) is by introducing acidic groups to form bridging hydrides. The

multiple Fe-centers in the  $E_4$  state may serve this role.<sup>6</sup> To model these intermediates with redox-inactive acids, we targeted the synthesis of ferrous-dihydride compounds in the presence of appended boron Lewis acids. Herein, we report Lewis acid enabled isolation of a high-spin Fe(II)-di(boro)hydride as well as its reduction product, an  $S = 3/2$  Fe-di(boro)hydride, and subsequent reactivity.

The complex,  $(^{BBN}PDP^{tBu})FeBr_2$ , contains a pair of moderately acidic 9-borabicyclo[3.3.1]nonyl (9-BBN) substituents that are capable of interacting with nitrogenous substrates independent of the metal center ( $N_2H_4$ ) or cooperatively with the metal center ( $NH_2^-$ ).<sup>7</sup> Treatment of a freshly-thawed orange THF solution of  $(^{BBN}PDP^{tBu})FeBr_2$  with two equiv. KBHET<sub>3</sub> affords an olive-tan powder, assigned as  $(^{BBN}PDP^{tBu})FeH_2$  (**1**) (70%, Fig. 2). **1** is modestly stable with a half-life of  $\sim 24$  h in THF at room temperature. Investigation by <sup>1</sup>H-NMR spectroscopy (THF) revealed a paramagnetically shifted spectrum with resonances ranging  $-16.9$ – $63.6$  ppm. The decrease in solution symmetry

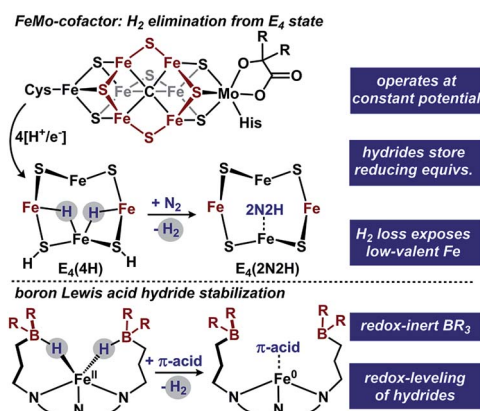


Fig. 1 FeMo-cofactor and our approach to hydride accumulation with boron Lewis acids.

<sup>a</sup>University of Michigan, 930 N. University, Ann Arbor, MI 48109, USA. E-mail: nszym@umich.edu

<sup>b</sup>H. C. Brown Laboratory, Purdue University, 560 Oval Dr, West Lafayette, IN 47907, USA

† Electronic supplementary information (ESI) available. CCDC 1884220–1884232 and 1903500. For ESI and crystallographic data in CIF or other electronic format see DOI: 10.1039/c9sc00561g

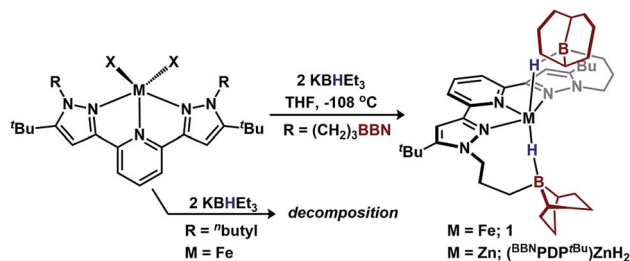


Fig. 2 Synthesis of borane-capped metal-dihydrides.

from  $C_{2v}$  to  $C_2$  is consistent with the trialkylboranes interacting with the hydride ligands at the Fe-center. Infrared spectroscopy (KBr) supported this formulation with a broad Fe–H–B stretch at  $\sim 1839\text{ cm}^{-1}$ .<sup>8</sup> Notably, the energy of this absorption is at significantly lower energy than bis(tris(mercaptoimidazolyl)hydroborato)-Fe(II) species that display a bridging borohydride.<sup>9</sup> Solution magnetic susceptibility studies (25 °C, THF) establish **1** as high-spin Fe(II) ( $\mu_{\text{eff}} = 4.6 \pm 0.2\ \mu_{\text{B}}$ ).

Single-crystal X-ray diffraction (XRD) experiments confirmed **1** as an iron-dihydride with each hydride capped by pyramidalized trialkylboranes (Fe–B = 2.970 Å;  $\sum \text{B}_\alpha = 318.6^\circ$ ;

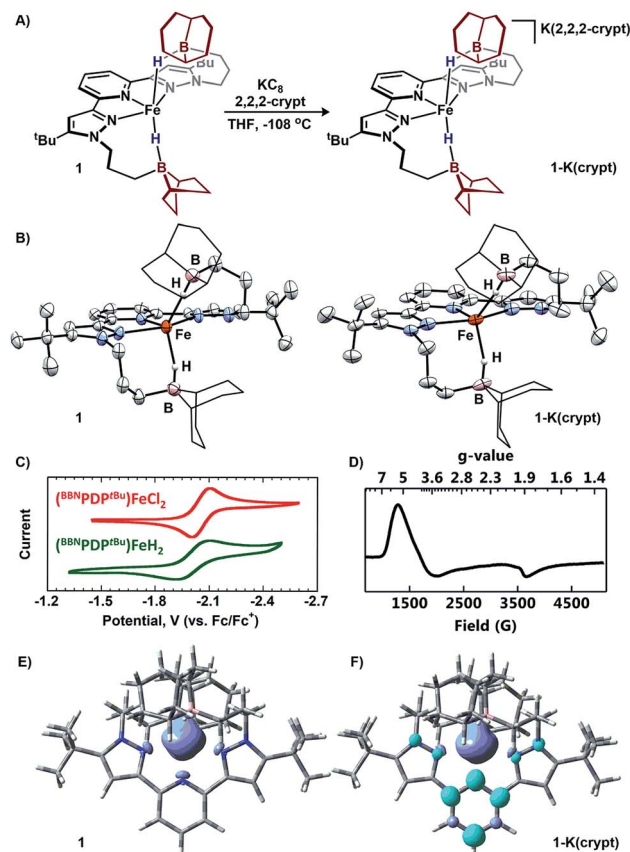


Fig. 3 (A) Reduction of **1**. (B) Molecular structures of **1** and **1-K(crypt)** (50% probability ellipsoids). For clarity, the 9-BBN substituents are displayed in wireframe. (C) Electrochemical comparison between **1** and  $(\text{BBN}\text{PDP}^t\text{Bu})\text{FeCl}_2$ . (D) X-band EPR of **1-K(crypt)** at 10 K in 1 : 1 toluene/THF. (E and F) Spin-density isosurface plots (0.002 a.u.) of **1** and **1-K(crypt)**, respectively.

Fig. 3B). The geometry about iron is best described as square pyramidal ( $\tau_5 = 0.31$ ). Complex **1** is a rare example of a mono-metallic high-spin Fe(II)-dihydride (or Fe(II)-diborohydride).<sup>1a,6c,9</sup>

The requirements of the intramolecular acids to stabilize **1** were assessed with a control ligand,  $\text{B}^{\text{Bu}}\text{PDP}^t\text{Bu}$ , where the  $-(\text{CH}_2)_3\text{BBN}$  fragments are replaced with *n*-butyl groups (Fig. 2).<sup>7</sup> Treating  $(\text{B}^{\text{Bu}}\text{PDP}^t\text{Bu})\text{FeBr}_2$  with 2 equiv.  $\text{KBHET}_3$  afforded intractable mixtures, precluding characterization (see ESI†). We propose that the appended trialkylboranes in **1** serve two important roles: (1) to stabilize the hydride ligands, and (2) to decrease the entropic penalty for stabilization (intramolecular 9-BBN vs. exogenous  $\text{BET}_3$ ). Attempts to install another donor ligand to **1** and enforce a low-spin configuration were unsuccessful: **1** was unreactive toward stoichiometric 1,4-diazabicyclo[2.2.2]octane,  $\text{NMe}_3$ , and  $\text{PMe}_3$ , but decomposed when treated with 4-dimethylaminopyridine.

To assess the requirements of the metal center and provide additional spectroscopic characterization, we synthesized the zinc analogue,  $(\text{BBN}\text{PDP}^t\text{Bu})\text{ZnH}_2$ , from  $(\text{BBN}\text{PDP}^t\text{Bu})\text{ZnI}_2$  (Fig. 2).  $^{11}\text{B}$ -NMR spectroscopy (THF) of  $(\text{BBN}\text{PDP}^t\text{Bu})\text{ZnH}_2$  revealed an upfield resonance at 5.43 ppm, consistent with a tetrahedral boron center.<sup>10</sup> IR spectroscopy (KBr) revealed a broad Zn–H–B stretch at  $\sim 1775\text{ cm}^{-1}$  that shifts upon deuterium labeling to  $\sim 1300\text{ cm}^{-1}$ .<sup>11</sup>  $^2\text{H}$ -NMR spectroscopy established the assignment of the hydride resonance at 0.65 ppm, which is comparable to other  $\kappa^1\text{-Zn}(\text{BH}_4)/\text{Zn}(\text{BH}_3\text{R})$  complexes.<sup>12</sup> The molecular structure of  $(\text{BBN}\text{PDP}^t\text{Bu})\text{ZnH}_2$  displays bonding metrics analogous to **1** (see ESI†).

Electrochemical investigation of **1** using cyclic voltammetry (0.2 M  $[\text{Bu}_4\text{N}][\text{PF}_6]$ , THF) revealed a quasi-reversible reductive event at  $-2.06\text{ V}$  vs.  $\text{Fc}/\text{Fc}^+$  which is minimally shifted from  $(\text{BBN}\text{PDP}^t\text{Bu})\text{FeCl}_2$  ( $\Delta = +10\text{ mV}$ ),<sup>13</sup> despite their different X-type donors (Fig. 3C).<sup>14</sup> The similar redox potentials suggest that, in analogy to the  $\text{E}_4$  state of nitrogenase, reducing equivalents can be delivered at a near constant potential to a Fe(II) state, when stored as bridging hydride equivalents.<sup>15</sup> To prepare the reduced complex, 1 equiv. of  $\text{KC}_8$  was added to a freshly thawed THF solution of **1** in the presence of 2,2,2-cryptand, resulting in an immediate color change to a vibrant green species assigned as  $[\text{K}(2,2,2\text{-cryptand})][(\text{BBN}\text{PDP}^t\text{Bu})\text{FeH}_2]$  (**1-K(crypt)**; Fig. 3A).<sup>16</sup> Investigation of **1-K(crypt)** by  $^1\text{H}$ -NMR spectroscopy (THF) revealed a paramagnetically shifted spectrum with resonances ranging  $-70.6$ – $95.0\text{ ppm}$  with solution  $C_2$  symmetry. Samples of **1-K(crypt)** are less stable than **1** and have an approximate half-life of 12 h in THF at room temperature. Upon reduction, the Fe–H–B infrared absorption shifts to higher energy ( $\sim 1866\text{ cm}^{-1}$ ; KBr). Solution magnetic susceptibility studies (25 °C, THF) of **1-K(crypt)** are consistent with an  $S = 3/2$  complex ( $\mu_{\text{eff}} = 4.1 \pm 0.1\ \mu_{\text{B}}$ ).<sup>17</sup> X-band EPR spectroscopy was employed to confirm the spin-state. Regardless of coordination environment or geometry,  $S = 1/2$  iron complexes, typically exhibit *g* values near the free electron value,<sup>18</sup> while high-spin complexes exhibit *g*<sub>x</sub>-tensors  $> 3.5$ .<sup>2,19</sup> **1-K(crypt)** displays a broad rhombic signal with *g* values of 5.6, 3.97, and 1.82 at 10 K in 1 : 1 THF/toluene glass (Fig. 3D), which suggests **1-K(crypt)** is best described as high-spin.<sup>20</sup> Reduced iron complexes with low coordination numbers (2, 3, occasionally 4) are often high-spin,<sup>19c,19e,21</sup> while

those stabilized by strong-field ligands (*i.e.* NHC, porphyrin, phosphines) are low-spin. **1-K(crypt)** is a rare example of a high-spin complex with a coordination number  $\geq 5$ .<sup>19b</sup>

For structural comparison, **1-K(crypt)** was examined by XRD. Data refinement revealed the anionic portion of **1-K(crypt)** to be geometrically similar ( $\tau_5 = 0.36$ ) to **1** (Fig. 3B). The interacting trialkylboranes are equidistant from the metal center in **1** and **1-K(crypt)**. Upon reduction, the Fe–N<sub>pyridine</sub> bond distance decreases from 2.178(5) to 2.021(6) consistent with enhanced  $\pi$ -backbonding.<sup>22</sup> DFT optimized geometries for the high-spin configuration of **1** and **1-K(crypt)** are in agreement with their crystallographic structures.<sup>23</sup> The spin-density for **1** is localized on iron, consistent with a high-spin Fe(II) description (Fig. 3E). For **1-K(crypt)**, significant spin-density is localized on the pyridyl-moiety of the chelate. The calculated  $\beta$ -SOMO for **1-K(crypt)** corresponding to reduction is primarily comprised of ligand- $\pi^*$  orbitals on the pyridyl moiety with minimal Fe contribution (19%). This analysis is consistent with reduction of **1** affording an  $S = 3/2$  system through antiferromagnetic coupling of high-spin Fe(II) with  $[\text{BBN}^{\text{PDP}^{\text{tBu}}}]^{1-}$ .<sup>24</sup> The calculated electronic structure is consistent with crystallographic bond metrics.<sup>25</sup> Pyridyl- $\pi^*$  population is reflected by C<sub>3</sub>–C<sub>4</sub> bond elongation (**1**: 1.377(6); **1-K(crypt)**: 1.433(12)<sub>ave</sub> Å; Fig. S85†).

We sought to examine the generality of the trialkylborane Lewis acids to stabilize both the accumulated hydrides and other small molecules. Addition of E–H substrates (E = NH<sub>2</sub>, NHMe, NHPH, OH, PPh, SPh) to freshly thawed THF solutions of **1** afford **2-E** as orange-tan powders with production of H<sub>2</sub> (Fig. 4).<sup>26</sup> **2-E** are high-spin Fe(II)-species with solution magnetic susceptibilities ranging  $\mu_{\text{eff}} = 4.5$ – $5.5 \mu_{\text{B}}$  (THF, 25 °C). **2-OH** and **2-PHPh** provide diagnostic infrared handles with sharp  $\nu_{\text{(OH)}}$ / $\nu_{\text{(PH)}}$  absorptions observed at 3630 and 2340 cm<sup>−1</sup> (KBr), respectively—each consistent with previously reported M–OH–BR<sub>3</sub><sup>27</sup> and Fe-phosphides.<sup>28</sup> <sup>1</sup>H-NMR spectroscopy revealed **2-NHMe**, **2-NHPH**, **2-OH**, and **2-PHPh** are C<sub>2</sub> symmetric in solution—consistent with Fe–E–B interactions remaining intact in solution. In contrast, **2-SPh** exhibits a solution C<sub>2v</sub> symmetric spectrum that broadens upon cooling to −80 °C, consistent with reversible B–S binding; likely a consequence of a weaker B–S interaction.<sup>29</sup> This observation was supported by DFT analyses. In contrast to the strong B–O interaction in **2-OH** (favored by ~10 kcal per mol per interaction), the calculated B–S interaction is thermodynamically disfavored by ~9 kcal per mol per interaction. In solution, the B–SPh binding equilibria in **2-SPh** were arrested by treating **2-SPh** with two equiv. NH<sub>3</sub>. Competitive binding with NH<sub>3</sub> afforded the ammonia-borane species, (<sup>BBN</sup>PDP<sup>tBu</sup>)Fe(SPh)<sub>2</sub>(NH<sub>3</sub>)<sub>2</sub> (**3**), highlighting the utility of moderately acidic groups to reversibly interact with small molecule substrates (Fig. 5).

To assess the structural similarities, **2-E** were examined by XRD (Fig. 4). Each displays a pentacoordinate iron best described as distorted square-pyramidal with interacting trialkylboranes. The B–heteroatom distances range from 1.592(2)–2.0504(19) Å following the trend B–OH < B–NHMe < B–NHPH < B–PPh = B–SPh. The same trend is observed for the Fe–heteroatom distance with **2-OH** displaying the shortest bond (1.9812(13) Å) and **2-PHPh**/**2-SPh** displaying the longest bond

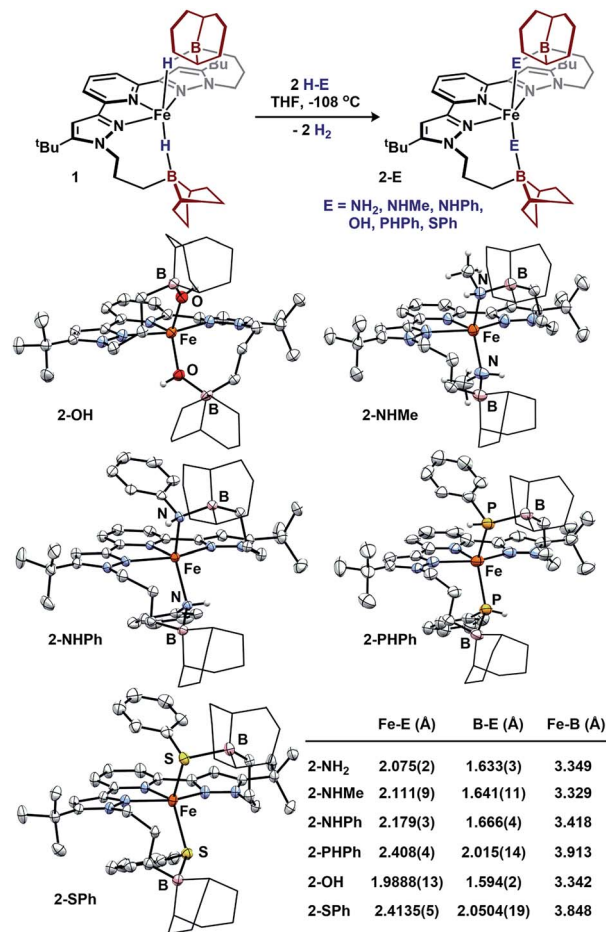


Fig. 4 Formation of **2-E** and molecular structures (50% probability ellipsoids) and averaged bond distances. For clarity, the 9-BBN substituents are displayed in wireframe.

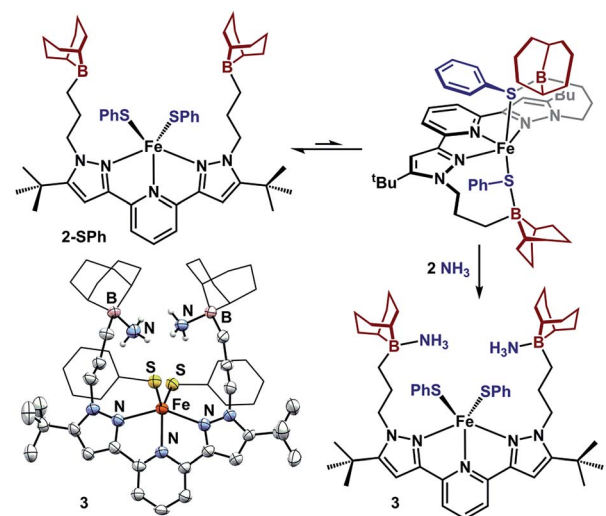


Fig. 5 Reversible acid/base interaction in **2-SPh** and molecular structure of **3** (50% probability ellipsoids). For clarity, the 9-BBN and phenyl substituents are displayed in wireframe.







This journal is © The Royal Society of Chemistry 2019

- R. M. Bullock, H<sub>2</sub> Binding, Splitting, and Net Hydrogen Atom Transfer at a Paramagnetic Iron Complex, *J. Am. Chem. Soc.*, 2019, **141**, 1871–1876.
- 2 R. Y. Igarashi, M. Laryukhin, P. C. Dos Santos, H.-I. Lee, D. R. Dean, L. C. Seefeldt and B. M. Hoffman, Trapping H-Bound to the Nitrogenase FeMo-Cofactor Active Site during H<sub>2</sub> Evolution: Characterization by ENDOR Spectroscopy, *J. Am. Chem. Soc.*, 2005, **127**, 6231–6241.
- 3 B. M. Hoffman, D. Lukoyanov, D. R. Dean and L. C. Seefeldt, Nitrogenase: A Draft Mechanism, *Acc. Chem. Res.*, 2013, **46**, 587–595.
- 4 (a) A. Jablonskytė, J. A. Wright, S. A. Fairhurst, J. N. T. Peck, S. K. Ibrahim, V. S. Oganessian and C. J. Pickett, Paramagnetic Bridging Hydrides of Relevance to Catalytic Hydrogen Evolution at Metallosulfur Centers, *J. Am. Chem. Soc.*, 2011, **133**, 18606–18609; (b) W. Wang, M. J. Nilges, T. B. Rauchfuss and M. Stein, Isolation of a Mixed Valence Diiron Hydride: Evidence for a Spectator Hydride in Hydrogen Evolution Catalysis, *J. Am. Chem. Soc.*, 2013, **135**, 3633–3639; (c) R. A. Kinney, C. T. Saouma, J. C. Peters and B. M. Hoffman, Modeling the Signatures of Hydrides in Metalloenzymes: ENDOR Analysis of a Di-iron Fe( $\mu$ -NH)( $\mu$ -H)Fe Core, *J. Am. Chem. Soc.*, 2012, **134**, 12637–12647; (d) J. M. Smith, R. J. Lachicotte and P. L. Holland, NN Bond Cleavage by a Low-Coordinate Iron(III) Hydride Complex, *J. Am. Chem. Soc.*, 2003, **125**, 15752–15753; (e) J. Rittle, C. C. L. McCrory and J. C. Peters, A 106-Fold Enhancement in N<sub>2</sub>-Binding Affinity of an Fe<sub>2</sub>( $\mu$ -H)<sub>2</sub> Core upon Reduction to a Mixed-Valence Fe<sup>II</sup>Fe<sup>I</sup> State, *J. Am. Chem. Soc.*, 2014, **136**, 13853–13862.
- 5 (a) E. W. Dahl, J. J. Kiernicki, M. Zeller and N. K. Szymczak, Hydrogen Bonds Dictate O<sub>2</sub> Capture and Release within a Zinc Tripod, *J. Am. Chem. Soc.*, 2018, **140**, 10075–10079; (b) E. W. Dahl, H. T. Dong and N. K. Szymczak, Phenylamino derivatives of tris(2-pyridylmethyl)amine: hydrogen-bonded peroxodicopper complexes, *Chem. Commun.*, 2018, **54**, 892–895; (c) C. M. Moore and N. K. Szymczak, Redox-induced fluoride ligand dissociation stabilized by intramolecular hydrogen bonding, *Chem. Commun.*, 2015, **51**, 5490–5492; (d) O. Tutusaus, C. Ni and N. K. Szymczak, A Transition Metal Lewis Acid/Base Triad System for Cooperative Substrate Binding, *J. Am. Chem. Soc.*, 2013, **135**, 3403–3406; (e) E. W. Dahl and N. K. Szymczak, Hydrogen Bonds Dictate the Coordination Geometry of Copper: Characterization of a Square-Planar Copper(I) Complex, *Angew. Chem., Int. Ed.*, 2016, **55**, 3101–3105.
- 6 (a) D.-H. Manz, P.-C. Duan, S. Dechert, S. Demeshko, R. Oswald, M. John, R. A. Mata and F. Meyer, Pairwise H<sub>2</sub>/D<sub>2</sub> Exchange and H<sub>2</sub> Substitution at a Bimetallic Dinickel(II) Complex Featuring Two Terminal Hydrides, *J. Am. Chem. Soc.*, 2017, **139**, 16720–16731; (b) K. J. Anderton, B. J. Knight, A. L. Rheingold, K. A. Abboud, R. García-Serres and L. J. Murray, Reactivity of hydride bridges in a high-spin [Fe<sub>3</sub>( $\mu$ -H)<sub>3</sub>]<sup>3+</sup> cluster: reversible H<sub>2</sub>/CO exchange and Fe–H/B–F bond metathesis, *Chem. Sci.*, 2017, **8**, 4123–4129; (c) Y. Yu, A. R. Sadique, J. M. Smith, T. R. Dugan, R. E. Cowley, W. W. Brennessel, C. J. Flaschenriem, E. Bill, T. R. Cundari and P. L. Holland, The Reactivity Patterns of Low-Coordinate Iron–Hydride Complexes, *J. Am. Chem. Soc.*, 2008, **130**, 6624–6638.
- 7 J. J. Kiernicki, M. Zeller and N. K. Szymczak, Hydrazine Capture and N–N Bond Cleavage at Iron Enabled by Flexible Appended Lewis Acids, *J. Am. Chem. Soc.*, 2017, **139**, 18194–18197.
- 8 (a) M. A. Nesbit, D. L. M. Suess and J. C. Peters, E–H Bond Activations and Hydrosilylation Catalysis with Iron and Cobalt Metalloboranes, *Organometallics*, 2015, **34**, 4741–4752; (b) D. L. M. Suess and J. C. Peters, H–H and Si–H Bond Addition to Fe $\equiv$ NNR<sub>2</sub> Intermediates Derived from N<sub>2</sub>, *J. Am. Chem. Soc.*, 2013, **135**, 4938–4941; (c) E. Alberico, P. Sponholz, C. Cordes, M. Nielsen, H.-J. Drexler, W. Baumann, H. Junge and M. Beller, Selective Hydrogen Production from Methanol with a Defined Iron Pincer Catalyst under Mild Conditions, *Angew. Chem., Int. Ed.*, 2013, **52**, 14162–14166; (d) R. Bau, H. S. H. Yuan, M. V. Baker and L. D. Field, An X-ray study of FeH(dmpe)<sub>2</sub>(BH<sub>4</sub>): a compound containing a singly-bridged BH<sub>4</sub> ligand with a bent Fe–H–B linkage, *Inorg. Chim. Acta*, 1986, **114**, L27–L28; (e) D. L. M. Suess and J. C. Peters, A CO-Derived Iron Dicarbyne That Releases Olefin upon Hydrogenation, *J. Am. Chem. Soc.*, 2013, **135**, 12580–12583.
- 9 (a) J. S. Figueroa, J. G. Melnick and G. Parkin, Reactivity of the Metal  $\rightarrow$  BX<sub>3</sub> Dative  $\sigma$ -Bond: 1,2-Addition Reactions of the Fe  $\rightarrow$  BX<sub>3</sub> Moiety of the Ferraboratrane Complex [ $\kappa^4$ -B(mimBut)<sub>3</sub>]Fe(CO)<sub>2</sub>, *Inorg. Chem.*, 2006, **45**, 7056–7058; (b) C. Kimblin, D. G. Churchill, B. M. Bridgewater, J. N. Girard, D. A. Quarless and G. Parkin, Tris(mercaptoimidazolyl)hydroborato complexes of cobalt and iron, [TmPh]<sub>2</sub>M (M=Fe, Co): structural comparisons with their tris(pyrazolyl)hydroborato counterparts, *Polyhedron*, 2001, **20**, 1891–1896; (c) See ESI Table S21† for further literature comparisons to Fe–B bond distances and  $\nu$ (Fe–H–B) vibrational data.
- 10 B–H coupling is not observed presumably due to low symmetry at boron.
- 11 Attempts at deuterium labeling **1** with LiBDEt<sub>3</sub> were unsuccessful.
- 12 S. Marks, R. Köppe, T. K. Panda and P. W. Roesky, Unprecedented Zinc–Borane Complexes, *Chem.–Eur. J.*, 2010, **16**, 7096–7100.
- 13 Potentials were assessed by square wave voltammetry.
- 14 A typical shift of 200–300 mV is expected per Cl/H substitution, see: (a) T. Liu, D. L. DuBois and R. M. Bullock, An iron complex with pendent amines as a molecular electrocatalyst for oxidation of hydrogen, *Nat. Chem.*, 2013, **5**, 228; (b) M. Tilset, I. Fjeldahl, J.-R. Hamon, P. Hamon, L. Toupet, J.-Y. Saillard, K. Costuas and A. Haynes, Theoretical, Thermodynamic, Spectroscopic, and Structural Studies of the Consequences of One-Electron Oxidation on the Fe–X Bonds in 17- and 18-Electron Cp\*Fe(dppe)X Complexes (X = F, Cl, Br, I, H, CH<sub>3</sub>), *J. Am. Chem. Soc.*, 2001, **123**, 9984–10000; (c) Y. Hu, L. Li, A. P. Shaw, J. R. Norton, W. Sattler and Y. Rong,





- 31 N. A. Eckert, J. M. Smith, R. J. Lachicotte and P. L. Holland, Low-Coordinate Iron(II) Amido Complexes of  $\beta$ -Diketiminates: Synthesis, Structure, and Reactivity, *Inorg. Chem.*, 2004, **43**, 3306–3321.
- 32 (a) R. D. Bemowski, A. K. Singh, B. J. Bajorek, Y. DePore and A. L. Odom, Effective donor abilities of E-*t*-Bu and EPh (E = O, S, Se, Te) to a high valent transition metal, *Dalton Trans.*, 2014, **43**, 12299–12305; (b) S. A. DiFranco, N. A. Maciulis, R. J. Staples, R. J. Batrice and A. L. Odom, Evaluation of Donor and Steric Properties of Anionic Ligands on High Valent Transition Metals, *Inorg. Chem.*, 2012, **51**, 1187–1200.
- 33 Analysis of the LUMO's were used in lieu of the optimized reduced complexes of **2-E** and truncated variants because (1) the reorganization of **1** upon reduction is minimal, (2) the high correlation between the  $\beta$ -LUMO of **1** and the  $\beta$ -SOMO of **1-K(crypt)**, see Fig. S88.† An analysis LUMO energies and calculated reduction potentials or a subset of **1** and **2-E** is included in the ESI.†
- 34 (a) D. D. Méndez-Hernández, J. G. Gillmore, L. A. Montano, D. Gust, T. A. Moore, A. L. Moore and V. Mujica, Building and testing correlations for the estimation of one-electron reduction potentials of a diverse set of organic molecules, *J. Phys. Org. Chem.*, 2015, **28**, 320–328; (b) J. R. Levin, W. L. Dorfner, A. X. Dai, P. J. Carroll and E. J. Schelter, Density Functional Theory as a Predictive Tool for Cerium Redox Properties in Nonaqueous Solvents, *Inorg. Chem.*, 2016, **55**, 12651–12659.
- 35 (a) R. Hoffmann, P. von Ragué Schleyer and H. F. Schaefer III, Predicting Molecules—More Realism, Please!, *Angew. Chem., Int. Ed.*, 2008, **47**, 7164–7167; (b) The truncated analogue, (<sup>Me</sup>PDP<sup>tBu</sup>)FeH<sub>2</sub>, is calculated to have a M–H bond index of 0.65.
- 36 The assignment of (<sup>BBN</sup>PDP<sup>tBu</sup>)Fe(CNAr)<sub>2</sub> is based on <sup>1</sup>H NMR and IR spectroscopies as well as MALDI mass spectrometry. We have been unable to isolate analytically pure samples of this species due to its high solubility.

